

## Vibrational Analysis of P<sub>4</sub>O<sub>6</sub> and P<sub>4</sub>O<sub>10</sub>

Richard C. Mowrey\* and Bradley A. Williams

Chemistry Division, Naval Research Laboratory, Washington, D.C. 20375

Charles H. Douglass

Nova Research, Inc., 1900 Elkin Street, Alexandria, Virginia 22308

Received: March 25, 1997; In Final Form: June 10, 1997<sup>⊗</sup>

The equilibrium geometries, vibrational frequencies, and infrared and Raman intensities for P<sub>4</sub>O<sub>6</sub> and P<sub>4</sub>O<sub>10</sub> were calculated using the Hartree–Fock self-consistent-field method. The computed geometries are in good agreement with experimental measurements. Scaling the *ab initio* vibrational frequencies of P<sub>4</sub>O<sub>10</sub> to account for anharmonicity and neglect of electron correlation yields values that agree with experimentally observed transitions, confirming the previous assignment of the spectrum. The energy ordering of the computed vibrational levels for P<sub>4</sub>O<sub>6</sub> differs, in part, from assignments based on experimental data. A new assignment that is in agreement with both the computations and the experiments is suggested; this requires the reassignment of four of the fundamental vibrations. The infrared emission spectrum produced by burning red phosphorus in air was recorded and the observed peaks assigned to P<sub>4</sub>O<sub>10</sub> transitions. The experimental relative intensities of the fundamental vibrations agree well with the computed relative intensities.

### Introduction

Investigation of the chemiluminescence of phosphorus and its compounds dates back to the seventeenth century.<sup>1</sup> It is only in more recent times, however, that the species responsible for the visible and ultraviolet emissions have been identified and the chemical mechanisms have begun to be elucidated.<sup>2</sup> A variety of spectroscopic techniques have been applied to phosphorus-containing materials. Laser and flash discharge experiments have been used to characterize gas phase PO and PO<sub>2</sub>.<sup>3–6</sup> Andrews and his co-workers have carried out low-temperature matrix experiments in which they assign infrared absorptions to more than two dozen species in the P–O–H system.<sup>7–14</sup> Data on the spectroscopy of the higher oxides including the stable species P<sub>4</sub>O<sub>6</sub> and P<sub>4</sub>O<sub>10</sub> are surprisingly sparse. Infrared absorption and Raman spectra of P<sub>4</sub>O<sub>6</sub> and P<sub>4</sub>O<sub>10</sub> at room temperature have been reported and vibrational assignments have been made for each molecule.<sup>15–18</sup> Konings *et al.* have measured the infrared spectrum of gas phase P<sub>4</sub>O<sub>10</sub> at elevated temperature.<sup>19</sup> Several researchers have applied theoretical methods to phosphorus-containing species. Jarrett-Sprague and co-workers have calculated the geometries and vibrational frequencies of PO<sub>2</sub>, P<sub>2</sub>O, and P<sub>4</sub>O using both *ab initio* and pseudopotential methods.<sup>20,21</sup> Lohr has used *ab initio* methods to determine the molecular geometries, energies, and vibrational frequencies of several P–O–H species.<sup>22–26</sup> Egdell and co-workers have examined electronic energy levels in P<sub>4</sub>O<sub>6</sub> and P<sub>4</sub>O<sub>10</sub> using *ab initio* methods,<sup>27</sup> and other groups have applied *ab initio* methods to the study of P<sub>4</sub>O<sub>6</sub>.<sup>28,29</sup>

This paper reports the results of theoretical and experimental studies of phosphorus oxides. Using *ab initio* methods, we have determined optimized molecular geometries for P<sub>4</sub>O<sub>6</sub> and P<sub>4</sub>O<sub>10</sub>. We have calculated the vibrational frequencies for these molecules using analytic second derivatives. Results of the calculations are used to suggest reinterpretation of the infrared spectrum of P<sub>4</sub>O<sub>6</sub>. Experimentally, we have produced phosphorus oxides by combustion of elemental red phosphorus under ambient atmospheric conditions. We have examined the combustion products by infrared emission spectroscopy and

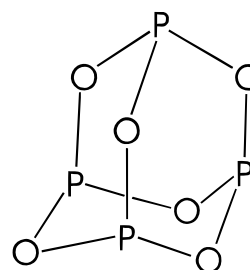


Figure 1. Geometry of P<sub>4</sub>O<sub>6</sub>.

assign the observed spectral features to vibrational modes of P<sub>4</sub>O<sub>10</sub>.

### Theoretical Method

Geometry optimization and vibrational analysis are performed at the Hartree–Fock self-consistent-field (SCF) level using the Gaussian 90 suite of commercial software.<sup>30</sup> The calculations are done with a double-zeta plus polarization (DZP) basis set. For oxygen, we use the Dunning 4s/2p contraction<sup>31</sup> of the 9s/5p primitive set of Huiznaga,<sup>32</sup> augmented by d polarization functions with an exponent of 0.85. The phosphorus DZP basis set is Dunning's 6s/4p contraction of Huiznaga's 11s/7p primitive set using d polarization functions with an exponent of 0.37. The DZP basis set has a total of 182 and 242 contracted basis functions for P<sub>4</sub>O<sub>6</sub> and P<sub>4</sub>O<sub>10</sub>, respectively. The effects of basis set size are studied by performing additional SCF calculations on P<sub>4</sub>O<sub>6</sub> using a minimal basis set (STO-3G) and a double-zeta basis set augmented with two sets of polarization functions on each atom (DZ2P). In the latter calculations, the exponents of the polarization functions on each oxygen atom are 1.7 and 0.425, and those on the phosphorus atoms are 0.74 and 0.185. Calculations on molecules of this size are computationally intensive due to the number of heavy atoms. Because of the large size of the basis sets, direct SCF calculations are performed in which the two-electron integrals are recomputed as needed rather than stored on disk. Minimum energy structures are located by gradient optimization using the Berny method.<sup>33</sup> Figure 1 shows the geometry used for P<sub>4</sub>O<sub>6</sub>. The

<sup>⊗</sup> Abstract published in *Advance ACS Abstracts*, July 15, 1997.

**TABLE 1: Calculated and Measured Bond Lengths and Angles for P<sub>4</sub>O<sub>6</sub> and P<sub>4</sub>O<sub>10</sub>**

	P <sub>4</sub> O <sub>6</sub>			P <sub>4</sub> O <sub>10</sub>	
	SCF theory	CISD theory	experiment <sup>34</sup>	SCF theory	experiment <sup>35</sup>
R(PO)	1.654 Å	1.664 Å	1.638 ± 0.003 Å	1.612 Å	1.604 ± 0.003 Å
R(PO) <sup>a</sup>				1.433 Å	1.429 ± 0.004 Å
∠(OPO)	98.69°	99.00°	99.8° ± 0.8°	100.6°	101.6° ± 0.8°
∠(OPO) <sup>a</sup>				117.1°	116.5° ± 0.3°
∠(POP)	128.2°	127.7°	126.7° ± 0.7°	125.3°	123.5° ± 0.7°

<sup>a</sup> Terminal oxygen atom.

**TABLE 2: Calculated Harmonic Vibrational Frequencies and Scaled Frequencies (cm<sup>-1</sup>), IR Intensities (km/mol), Raman Intensities (Å<sup>4</sup>/amu), and Symmetries for P<sub>4</sub>O<sub>10</sub> and Experimental Frequencies (cm<sup>-1</sup>) Observed in Infrared and Raman Spectra; Some Authors use T<sub>1</sub> and T<sub>2</sub> rather than F<sub>1</sub> and F<sub>2</sub> as Labels for Triply Degenerate Modes**

SCF frequency	theory			experiment			
	scaled frequency	infrared intensity	Raman intensity	Beattie <i>et al.</i> <sup>16</sup>	Konings <i>et al.</i> <sup>19</sup>	Chapman <sup>15</sup>	symmetry
258.8	243.8	0	3.93	254		258	E
277.2	261.1	0	0				F <sub>1</sub>
279.4	263.2	26.9	1.29	264	270.0	278	F <sub>2</sub>
351.6	331.7	0	0.01				E
431.0	406.0	31.9	3.55	411	409.0	424	F <sub>2</sub>
435.7	410.4	0	0				F <sub>1</sub>
572.7	539.5	0	16.5	553		556	A <sub>1</sub>
626.5	590.2	25.5	0.60		575.3	573	F <sub>2</sub>
795.5	749.4	0	12.5	717		721	A <sub>1</sub>
825.4	777.5	277.2	0.10		763.7	760	F <sub>2</sub>
881.4	830.3	0	1.59				E
925.7	872.0	0	0				F <sub>1</sub>
1114	1049	780.7	0.17		1012	1010	F <sub>2</sub>
1483	1397	569.5	6.18	1406	1404	1390	F <sub>2</sub>
1517	1429	0	28.1	1440		1413	A <sub>1</sub>

phosphorus atoms are constrained to be tetrahedral, and the oxygen atoms are at the vertices of an octahedron with each oxygen atom equidistant from its two neighboring phosphorus atoms. Since the bond angles are fixed at the values appropriate for *T<sub>d</sub>* symmetry, there are only two independent variables to be optimized for P<sub>4</sub>O<sub>6</sub>. The shape of P<sub>4</sub>O<sub>10</sub> is the same as P<sub>4</sub>O<sub>6</sub> with terminal oxygen atoms added to each of the phosphorus atoms. The distance from the phosphorus atoms to the terminal oxygen atoms adds a third coordinate. Vibrational frequencies are computed with the SCF method at the stable geometries using analytic second derivatives. For comparison purposes, a geometry optimization of P<sub>4</sub>O<sub>6</sub> is performed using the configuration interaction method including all single and double excitations (CISD) from the valence orbitals in the Hartree–Fock determinant. The calculations are carried out on a Silicon Graphics Indigo workstation.

### Experimental Method

Approximately 1 g samples of elemental red phosphorus (supplied by Strem Chemicals) are burned in air following hot wire ignition. The samples are contained in porcelain crucibles, which shield the spectrometer from the direct emission of the visible flame. Infrared emission spectra of the combustion plume are collected using a Mattson Instruments Cygnus 100 Fourier transform infrared spectrometer. For each spectrum, 32 scans collected at 1 cm<sup>-1</sup> resolution are coadded and Fourier processed.

### Theoretical Results

Computed bond lengths and bond angles of the minimum energy geometries for P<sub>4</sub>O<sub>6</sub> and P<sub>4</sub>O<sub>10</sub> using the DZP basis set are given in Table 1. Measured bond lengths and angles from electron diffraction studies of gaseous P<sub>4</sub>O<sub>6</sub> and P<sub>4</sub>O<sub>10</sub> are given for comparison.<sup>34,35</sup> The results in Table 1 show good agreement between theory and experiment and are consistent with previous theoretical treatments of P<sub>4</sub>O<sub>6</sub>.<sup>28,29</sup> For most values,

the results of the calculations are within the experimental uncertainty (estimated standard deviation) reported for the experiments or nearly so. The calculated geometries of P<sub>4</sub>O<sub>6</sub> and P<sub>4</sub>O<sub>10</sub> are similar with a slightly longer PO bond length in P<sub>4</sub>O<sub>6</sub>. The distances of the P and O atoms from the center of the P<sub>4</sub>O<sub>6</sub> molecule are 1.822 and 1.774 Å, respectively, compared to values of 1.752 and 1.754 Å for the slightly smaller kernel of the P<sub>4</sub>O<sub>10</sub> molecule. Geometries calculated for P<sub>4</sub>O<sub>6</sub> at the SCF and CISD levels are similar. The PO bond lengthens slightly in the CISD calculation due to correlation effects, increasing the difference between the experimental and calculated values. The rotational constants are calculated using the optimized DZP geometries. The rotational constant for P<sub>4</sub>O<sub>10</sub> is 0.019 cm<sup>-1</sup>, in agreement with the experimental value;<sup>19</sup> the rotational constant for P<sub>4</sub>O<sub>6</sub> is 0.035 cm<sup>-1</sup>.

The results of theoretical calculations of the harmonic vibrational frequencies and intensities of P<sub>4</sub>O<sub>10</sub> are compared with experimental observations in Table 2. Association of the calculated frequencies with the observed experimental frequencies is straightforward for P<sub>4</sub>O<sub>10</sub>, since the symmetry calculated for each transition corresponds to that assigned based on experimental data. The positions of the five highest frequency F<sub>2</sub> modes agree with the infrared spectra observed by McCluskey and Andrews in cryogenic matrices.<sup>11,13</sup> Vibrational frequencies computed using the SCF method are larger than those observed experimentally, as is typically the case. Better agreement between the calculated frequencies and the observations results from multiplying the calculated values by a scaling factor. In previous work on phosphorus oxides, Lohr derived a scaling factor of 0.868 based on the observed and calculated frequencies of PO.<sup>22</sup> We calculate the scaling factor by averaging the ratio of the experimental frequency to the computed frequency. When multiple experimental values are reported, the average of those values is used for calculating the scaling factor. The second column of Table 2 lists scaled frequency values obtained by multiplying the computed frequencies by our scaling factor

**TABLE 3: Calculated Harmonic Vibrational Frequencies and Scaled Frequencies (cm<sup>-1</sup>), IR Intensities (km/mol), Raman Intensities (Å<sup>4</sup>/amu), and Symmetries for P<sub>4</sub>O<sub>6</sub> and Experimental Frequencies (cm<sup>-1</sup>) Observed in Infrared and Raman Spectra**

theory				experiment		
SCF frequency	scaled frequency	infrared intensity	Raman intensity	Beattie <i>et al.</i> <sup>16</sup>	Chapman <sup>15</sup>	symmetry
311.2	288.4	0	0		285	F <sub>1</sub>
324.2	300.5	0	1.87	305	302	E
436.5	404.6	36.1	2.51	408	407	F <sub>2</sub>
607.2	562.8	1.0	0.09	562	549	F <sub>2</sub>
666.5	617.7	0	26.57	620	613	A <sub>1</sub>
696.5	645.5	92.9	5.51	642	643	F <sub>2</sub>
711.4	659.3	0	1.09		691	E
731.1	677.6	0	0		702	F <sub>1</sub>
796.8	738.5	0	1.35		718	A <sub>1</sub>
1058.3	980.8	913.5	1.63	959	919	F <sub>2</sub>

of 0.942. There are two differences between the ordering of the frequencies based on our results and that of Chapman based on force constant calculations.<sup>15</sup> These differences are in the ordering of the two lowest frequency F<sub>1</sub>, F<sub>2</sub> pairs. As will be discussed below, the computed frequencies and IR intensities are able to account for the infrared emissions from the combustion plume of elemental red phosphorus.

The computed harmonic vibrational frequencies and infrared and Raman intensities for P<sub>4</sub>O<sub>6</sub> are given in Table 3 along with the experimental infrared and Raman frequencies. The symmetry of each frequency is taken from the calculation and differs in some cases from the assignment based on the experimental data, as will be discussed below. We tested the effect of basis set selection on the calculated vibrational frequencies of P<sub>4</sub>O<sub>6</sub> by repeating the calculations with an STO-3G basis set and a DZ2P basis set. The STO-3G vibrational frequencies are scattered above and below the DZP frequencies with an average difference of 8.0%, and the order of the highest F<sub>1</sub> and A<sub>1</sub> levels is reversed. There is no substantial difference between the energies calculated with the DZP and DZ2P basis sets—the DZ2P values are ~1.6% higher—and there are no changes in the frequency ordering.

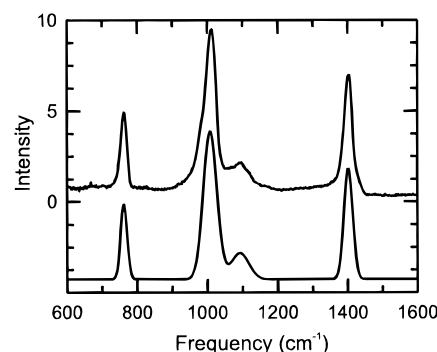
The fundamental vibrations of the P<sub>4</sub>O<sub>6</sub> molecule are represented by

$$\Gamma = 2A_1 + 2E + 2F_1 + 4F_2$$

Chapman assigned the frequencies of the fundamental vibrations on the basis of infrared and Raman spectra.<sup>15</sup> Beattie *et al.* followed Chapman's assignments for their Raman data.<sup>16</sup> The results of our calculations require that these assignments be re-examined. Chapman observed very strong or very, very strong infrared transitions at 407, 643, and 919 cm<sup>-1</sup>, and these modes are also Raman active, giving unpolarized bands. They are assigned as F<sub>2</sub> fundamentals. Chapman assigned the 302 cm<sup>-1</sup> band as the fourth F<sub>2</sub> mode, but our calculations rule out this assignment. From the symmetry of the calculated frequencies, we assign the lowest frequency mode at 285 cm<sup>-1</sup> as an F<sub>1</sub> mode and the 302 cm<sup>-1</sup> transition as type E. The most intense Raman transition is at 613 cm<sup>-1</sup> and is polarized; this is an A<sub>1</sub> mode. Chapman assigned the transition at 569 cm<sup>-1</sup> as an A<sub>1</sub> fundamental; we believe it is the first overtone of the 285 cm<sup>-1</sup> fundamental. The remaining F<sub>2</sub> mode is assigned to the 549 cm<sup>-1</sup> line; the low intensity of the line agrees with the small intensity predicted by the calculation. We are in accord with Chapman's assignment of the 691 cm<sup>-1</sup> line as an E-type mode. Using the scaled frequencies as a guide, we assign the remaining F<sub>1</sub> and A<sub>1</sub> fundamentals to the observed transitions at 702 and at 718 cm<sup>-1</sup>. With these assignments, the scaling factor for

**TABLE 4: Previous and Current Assignments for P<sub>4</sub>O<sub>6</sub> Transitions**

frequency (cm <sup>-1</sup> )	previous assignment <sup>15</sup>	current assignment
285	E fundamental	F <sub>1</sub> fundamental
302	F <sub>2</sub> fundamental	E fundamental
549	unassigned	F <sub>2</sub> fundamental
569	A <sub>1</sub> fundamental	285 + 285 = 570
702	302 + 407 = 709	F <sub>1</sub> fundamental
718	unassigned	A <sub>1</sub> fundamental
832	F <sub>1</sub> fundamental	285 + 549 = 834
1180	919 + 302 = 1221	549 + 643 = 1192
1460	832 + 643 = 1475	919 + 549 = 1468
1625	832 + 832 = 1664	919 + 702 = 1621

**Figure 2.** (Upper) The emission spectrum of the combustion plume of elemental red phosphorus burning in air. (Lower) Fit to the experimental data. The lower trace is offset by five units for clarity.**TABLE 5: Assignment of Labels to Fundamental Frequencies for P<sub>4</sub>O<sub>10</sub>**

label	frequency (cm <sup>-1</sup> )	label	frequency (cm <sup>-1</sup> )	label	frequency (cm <sup>-1</sup> )
$\nu_1$	1413 <sup>a</sup>	$\nu_6$	254 <sup>c</sup>	$\nu_{11}$	1012 <sup>d</sup>
$\nu_2$	721 <sup>a</sup>	$\nu_7$	872 <sup>b</sup>	$\nu_{12}$	764 <sup>d</sup>
$\nu_3$	556 <sup>a</sup>	$\nu_8$	410 <sup>b</sup>	$\nu_{13}$	575 <sup>d</sup>
$\nu_4$	830 <sup>b</sup>	$\nu_9$	261 <sup>b</sup>	$\nu_{14}$	409 <sup>d</sup>
$\nu_5$	332 <sup>b</sup>	$\nu_{10}$	1404 <sup>d</sup>	$\nu_{15}$	270 <sup>d</sup>

<sup>a</sup> Reference 15. <sup>b</sup> Scaled calculated frequency from this work.

<sup>c</sup> Reference 16. <sup>d</sup> Reference 19.

P<sub>4</sub>O<sub>6</sub> is 0.927. The data in Table 3 reflect the proposed changes in the assignment. The differences between our assignment and Chapman's assignment are summarized in Table 4.

## Experimental Results

The infrared emission spectrum of the combustion plume of elemental red phosphorus in air is shown as the upper trace in Figure 2. The plotted spectrum is the average of three measurements. Comparison of the spectrum with the data of Konings *et al.*<sup>19</sup> and with the results of our theoretical calculations allows us to assign the observed features to emission by P<sub>4</sub>O<sub>10</sub>. We label the P<sub>4</sub>O<sub>10</sub> transitions by grouping them by symmetry type and assigning the lowest number to the highest frequency within a set of transitions of the same symmetry.<sup>36</sup> This convention differs from the one used by Konings *et al.* The labels assigned to the fundamental frequencies are listed in Table 5. The three main peaks in the experimental spectrum are assigned to the three fundamental F<sub>2</sub> vibrations with the largest calculated infrared intensities. To the best of our knowledge, this is the first assignment of infrared emissions to P<sub>4</sub>O<sub>10</sub> produced in a reacting system. Table 6 presents the peak positions from the experimental spectrum and the calculated frequencies of the transitions scaled by 0.942.

Konings *et al.*<sup>19</sup> assigned the shoulder on the high-wavenumber side of the central peak to the first overtone of  $\nu_3$  (556

**TABLE 6: Experimental and Calculated Peak Positions and Assignments for the Emission Spectrum of the Combustion Plume of Elemental Red Phosphorus Burning in Air**

experimental frequency (cm <sup>-1</sup> ) <sup>19</sup>	scaled calculated frequency (cm <sup>-1</sup> )	assignment
764	778	$\nu_{12}$
1012	1049	$\nu_{11}$
1404	1397	$\nu_{10}$

**TABLE 7: Combination Bands That May Be Assigned to the Shoulder on the High-Wavenumber Side of the Central Peak in the Emission Spectrum**

bands	frequencies
$\nu_4 + \nu_6$	830 cm <sup>-1</sup> + 254 cm <sup>-1</sup> = 1084 cm <sup>-1</sup>
$\nu_4 + \nu_9$	830 cm <sup>-1</sup> + 261 cm <sup>-1</sup> = 1091 cm <sup>-1</sup>
$\nu_5 + \nu_{12}$	330 cm <sup>-1</sup> + 764 cm <sup>-1</sup> = 1094 cm <sup>-1</sup>
$\nu_4 + \nu_{15}$	830 cm <sup>-1</sup> + 270 cm <sup>-1</sup> = 1100 cm <sup>-1</sup>

**TABLE 8: Parameters for the Fit to the Spectrum Shown in Figure 2 and Experimental and Theoretical Relative Intensities for the Fundamental Vibrations in the Emission Spectrum**

transition	fit parameters			relative intensity		
	amplitude	line width (cm <sup>-1</sup> )	center frequency (cm <sup>-1</sup> )	integration range (cm <sup>-1</sup> )	calculation	experiment
$\nu_{12}$	4.10	13.3	762	700–800	3.6	3.2
$\nu_{11}$	8.14	27.2	1009	900–1100	10.0	10.0
combination	1.45	35.5	1093			
$\nu_{10}$	6.09	17.7	1402	1350–1500	7.3	5.6

cm<sup>-1</sup>), the A<sub>1</sub> mode that gives the most intense peak in the Raman spectrum. The overtone of this totally symmetric mode has A<sub>1</sub> symmetry and therefore is not infrared active. We propose that this shoulder with its maximum intensity at 1093 cm<sup>-1</sup> is a combination band. The bands listed in Table 7 fall into the correct frequency range and each has a component with F<sub>2</sub> symmetry, making it infrared allowed. We do not have sufficient information to choose among these possibilities.

In order to calculate the relative intensities of the three fundamental transitions from the experimental data, we must separate the  $\nu_{11}$  peak from the combination band. To extract the strength of an infrared transition from emission data, the spectrum is first divided by the Planck function  $\nu^3/(e^{h\nu/kT} - 1)$  at the temperature of the emitting species;<sup>37</sup> the plume is assumed to be optically thin. The temperature of the region of the flame where spectra were recorded is ~900 K, as measured by a thermocouple. After normalizing for the temperature, we fit the spectrum to a function that is the sum of four Gaussians, one for each observed peak, plus an additional parameter for the offset from zero. Each Gaussian is represented by the following functional form:

$$\sigma(\bar{\nu}) = A e^{-(\bar{\nu}-\bar{\nu}_0)^2/B^2}$$

where  $A$  = amplitude,  $B$  = line width, and  $\bar{\nu}_0$  = center frequency.

The amplitudes, line widths, and center frequencies of each peak are allowed to vary freely; the fit parameters are given in Table 8. The resulting fit, offset by five units for clarity, is plotted as the lower trace in Figure 2. We estimate the relative intensities by integrating the Gaussians individually and comparing these relative intensities to the theoretical results. Table 8 reports the relative intensities from the calculations and from the experiment, along with the frequency range over which the functional fit was integrated to determine the experimental intensities. The agreement between the calculations and the experiments is remarkably good.

## Summary

We have calculated the minimum energy geometries, vibrational frequencies, and infrared and Raman intensities at the SCF level for P<sub>4</sub>O<sub>6</sub> and P<sub>4</sub>O<sub>10</sub>. The bond lengths and bond angles compare well with the experimental values. The calculated fundamental frequencies for P<sub>4</sub>O<sub>10</sub> agree with the experimentally measured transitions. For P<sub>4</sub>O<sub>6</sub>, the assignment is not straightforward. On the basis of our calculations, we suggest a modified vibrational assignment that reassigns four fundamentals. We measured the infrared emission spectrum produced by burning elemental red phosphorus in air. The three peaks plus a shoulder in the spectrum can be assigned to transitions of P<sub>4</sub>O<sub>10</sub>; the relative experimental intensities are compared with those derived from the calculations. This is the first observation of infrared emission from P<sub>4</sub>O<sub>10</sub> formed in a reacting system.

**Acknowledgment.** The authors wish to thank Dr. H. D. Ladouceur for helpful discussions and assistance with the calculations. This work was supported in part by the Offboard IR/EO Countermeasures Task Area of the 6.2 Electronic Warfare Program of the Office of Naval Research. The work at NRL was supported by the Office of Naval Research through the Naval Research Laboratory.

## References and Notes

- (1) Harvey, E. N. *A History of Luminescence*; American Philosophical Society: Philadelphia, 1957.
- (2) Hamilton, P. A.; Murrells, T. A. *J. Phys. Chem.* **1986**, *90*, 182.
- (3) Butler, J. E.; Kawaguchi, K.; Hirota, E. *J. Mol. Spectrosc.* **1983**, *101*, 161.
- (4) Verma, R. D.; McCarthy, C. F. *Can. J. Phys.* **1983**, *61*, 1149.
- (5) Kawaguchi, K.; Saito, S.; Hirota, E.; Ohashi, N. *J. Chem. Phys.* **1985**, *82*, 4893.
- (6) Qian, H.; Davies, P. B.; Hamilton, P. A. *J. Chem. Soc., Faraday Trans.* **1995**, *91*, 2993.
- (7) Withnall, R.; Andrews, L. *J. Phys. Chem.* **1987**, *91*, 784.
- (8) Withnall, R.; Andrews, L. *J. Phys. Chem.* **1988**, *92*, 4610.
- (9) Andrews, L.; Withnall, R. *J. Am. Chem. Soc.* **1988**, *110*, 5605.
- (10) Mielke, Z.; McCluskey, M.; Andrews, L. *Chem. Phys. Lett.* **1990**, *165*, 146.
- (11) McCluskey, M.; Andrews, L. *J. Phys. Chem.* **1991**, *95*, 2679.
- (12) McCluskey, M.; Andrews, L. *J. Phys. Chem.* **1991**, *95*, 2988.
- (13) McCluskey, M.; Andrews, L. *J. Phys. Chem.* **1991**, *95*, 3545.
- (14) Andrews, L.; Mielke, Z. P.; Taylor, R.; Martin, J. M. L. *J. Phys. Chem.* **1994**, *98*, 10706.
- (15) Chapman, A. C. *Spectrochim. Acta* **1968**, *24A*, 1687.
- (16) Beattie, I. R.; Livingston, K. M. S.; Ozin, G. A.; Reynolds, D. J. *J. Chem. Soc. A* **1970**, 449.
- (17) Gerding, H.; Brederode, H. V.; De Decker, H. C. *J. Recl. Trav. Chim.* **1942**, *61*, 549.
- (18) Gerding, H.; De Decker, H. C. *J. Recl. Trav. Chim.* **1945**, *64*, 191.
- (19) Konings, R. J. M.; Cordfunke, E. H. P.; Booi, A. S. *J. Mol. Spectrosc.* **1992**, *152*, 29.
- (20) Jarrett-Sprague, S. A.; Hillier, I. H.; Gould, I. R. *Chem. Phys.* **1990**, *140*, 27.
- (21) Jarrett-Sprague, S. A.; Hillier, I. H. *Chem. Phys.* **1990**, *148*, 325.
- (22) Lohr, L. L. *J. Phys. Chem.* **1984**, *88*, 5569.
- (23) Lohr, L. L. *J. Phys. Chem.* **1990**, *94*, 1807.
- (24) Lohr, L. L. *J. Phys. Chem.* **1990**, *94*, 4832.
- (25) Lohr, L. L. *J. Phys. Chem.* **1992**, *96*, 119.
- (26) Lohr, L. L.; Boehm, R. C. *J. Phys. Chem.* **1991**, *91*, 3202.
- (27) Egdell, R. E.; Palmer, M. H.; Findlay, R. H. *Inorg. Chem.* **1980**, *19*, 1314.
- (28) Rose, J. L.; VanCott, T. C.; Schatz, P. N.; Boyle, M. E.; Palmer, M. H. *J. Phys. Chem.* **1989**, *93*, 3504.
- (29) Mühlhäuser, M.; Engels, B.; Marian, C. M.; Peyerimhoff, S. D.; Bruna, P. J.; Jansen, M. *Angew. Chem., Int. Ed. Engl.* **1994**, *33*, 563.
- (30) Frisch, M. J.; Head-Gordon, M.; Trucks, G. W.; Foresman, J. B.; Schlegel, H. B.; Raghavachari, K.; Robb, M. A.; Binkley, J. S.; Gonzalez, C.; Defrees, D. J.; Fox, D. J.; Whiteside, R. A.; Seeger, R.; Melius, C. F.; Baker, J.; Martin, R. L.; Kahn, L. R.; Stewart, J. J. P.; Topiol, S.; Pople, J. A. *Gaussian 90*; Gaussian, Inc.: Pittsburgh, 1990.

(31) Dunning, T. H.; Hays, P. J. In *Modern Theoretical Chemistry, Vol. 3. Methods of Electronic Structure Theory*; Schaefer, H. F., III, Ed.; Plenum Press: New York, 1977.

(32) Huizinaga, S. *J. Phys. Chem.* **1965**, *42*, 1293.

(33) Schlegel, H. B. *J. Comput. Chem.* **1982**, *3*, 214.

(34) Beagley, B.; Cruikshank, D. W. J.; Hewitt, T. G.; Jost, K. H. *Trans. Faraday Soc.* **1969**, *65*, 1219.

(35) Beagley, B.; Cruikshank, D. W. J.; Hewitt, T. G.; Haaland, A. *Trans. Faraday Soc.* **1967**, *63*, 836.

(36) Herzberg, G. *Molecular Spectra and Molecular Structure. II. Infrared and Raman Spectra of Polyatomic Molecules*; Van Nostrand: New York, 1945; p 163.

(37) Rybicki, G. B.; Lightman, A. P. *Radiative Processes in Astrophysics*; Wiley: New York, 1979; pp 1–50.